SENSITIVITY ANALYSIS OF THE ULTRASONIC RESPONSE FROM A NON-NORMAL SURFACE-BREAKING CRACK

A. Minachi, F. J. Margetan and R. B. Thompson
Center for NDE, Iowa State University
Ames, Iowa 50011

M. S. Greenwood
Pacific Northwest Laboratory
Richland, Washington 99352

INTRODUCTION

The use of computer simulations is becoming an increasing popular strategy for designing ultrasonic inspections. There are many benefits of accurate simulations, the most important one being their cost effectiveness. In many cases, before inspection procedures are finalized, it is possible to simulate the competing inspection plans, and to use the outputs of simulation trials to choose the best plan. This strategy is particularly useful when there is limited accessibility to the components that need to be inspected, as in the extreme case when the inspection procedure requires that operating equipment be removed from service. In such cases, it is best to be fully prepared before taking the inspection equipment to the test site and computer simulations can play an important role in such preparation, often at a significantly reduced cost with respect to traditional methods.

At the Center for Nondestructive Evaluation at Iowa State University, models have been developed to simulate a variety of inspection problems. One group of models, designed to aid in the inspection of nuclear power plants, predicts the ultrasonic response from surface-breaking cracks [1-3]. The cracks are assumed to be located on the side "opposite" to the sound entry surface, for example, on the inner surface of a pipe that is inspected using a transducer placed on its outer wall. These crack models have been primarily validated for cases in which the crack breaks the surface at normal incidence. However, in practice, the cracks could grow at other angles, and there was a need to develop and validate models for non-normal surface cracks.

Dr. Margaret Greenwood at Pacific Northwest Laboratory, who was endeavoring to test the crack models, noticed the strong sensitivity of the predicted crack response to the assumed crack angles. Furthermore, she found that certain predictions of the models appeared to disagree with common sense. For example, the simulations indicated that for a 45° longitudinal-wave or shear-wave inspection, the peak crack response (regarded as a function of crack tilt angle) did not occur when the crack was normal to the surface. Her results prompted a more in-depth study of the sensitivity of the ultrasonic crack response to the crack angle. In this paper, model predictions for non-normal, surface-breaking cracks are compared with experiment, and the principal findings are summarized and discussed.

THEORETICAL BACKGROUND

Ultrasonic Response from a Crack (Via Auld's Reciprocity Relation)

To predict the electric voltage signal which arises from the backscattering of an ultrasonic beam from a crack, Auld's reciprocity formula [4] is used. In that formula, Auld

Review of Progress in Quantitative Nondestructive Evaluation, Vol 16
Edited by D.O. Thompson and D.E. Chimenti, Plenum Press, New York, 1997

introduced an electromagnetic reflection coefficient Γ which is directly proportional to the strength of the field produced in the coaxial "output" cable. Then, for a nonpiezoelectric elastic media and general pitch-catch geometry, he derived a relationship for the change in Γ that is produced by the present of a flaw. For a pulse/echo inspection this reduces to:

$$\Gamma_{flaw} - \Gamma_{no\ flaw} = \frac{1}{4P} \int_S (\mathbf{V}_1 \cdot \mathbf{T}_2 - \mathbf{V}_2 \cdot \mathbf{T}_1) \cdot \vec{n}\, dS \quad . \tag{1}$$

In the above equation, P is the input electrical power supplied to the transducer, and $\mathbf{V}_1$ and $\mathbf{T}_1$ are the complex amplitudes of the time-harmonic velocity and stress fields which occur in the absence of the flaw. $\mathbf{V}_2$ and $\mathbf{T}_2$ are the fields which would occur in the presence of the flaw under the same conditions. The Vector $\vec{n}$ is an outward normal vector to the integration surface, S, which can be any surface enclosing the flaw. We choose S to be the crack surface itself. Since the net stress must vanish on the surface of the crack, $\mathbf{T}_2 \cdot \vec{n}$ is equal to zero in the integrand of Eq. (1), and the equation reduces to

$$\Gamma_{flaw} - \Gamma_{no\ flaw} = \frac{-1}{4P} \int_S \mathbf{V}_2 \cdot \mathbf{T}_1 \cdot \vec{n}\, dS \quad . \tag{2}$$

As shown in Figure 1, each point on the surface of the crack is illuminated by both a "direct" field that has passed through the top interface of the component containing the crack and a "secondary" field reflected from the bottom interface.

To evaluate the integrand of Eq. (2), the Kirchhoff approximation is used for the scattered fields. This approximation assumes that the total field is negligible at points on the "far" (non-illuminated) side of the crack face. On the near side of the crack, the total field is obtained by summing the incident field and the scattered field that is produced when that incident field is reflected by the crack. Note that the field incident on the crack has two components, the direct field and that reflected by the bottom interface. The scattering from both components must be calculated. For either component under the Kirchhoff approximation, the scattered field at a point on the crack face is obtained by treating the incident filed there as a local plane wave, and applying the usual rules for reflection of a plane wave by a flat interface. In summary, the incident stress field $\mathbf{T}_1$ has two contributions (the direct field and one reflected from the bottom interface) and the total field $\mathbf{V}_2$ has four contributions (direct and reflected incident fields, and their reflections by the crack face). The Kirchhoff approximation accurately describes the specular reflection when the crack is significantly larger that the sonic wavelength. However, the tip diffracted signal is not calculated correctly. Therefore, care should be taken to insure that when the model is applied, the probe location and tilt angle of the crack (θ in Fig. 2) are such that specular reflection dominates the tip diffracted contribution to the crack response.

Incident Beam Evaluation

To compute the integrand of Eq. (2) under the Kirchhoff approximation, the complex amplitudes of the incident time-harmonic velocity and stress fields must be first found

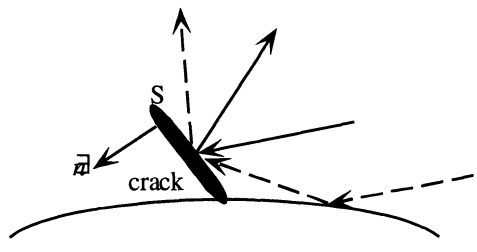

Figure 1. A surface-breaking crack being illiminated by a beam originating above and to the right of the crack. The crack is illuminated by both direct rays (solid lines) and rays reflected from the lower surface (dashed lines).

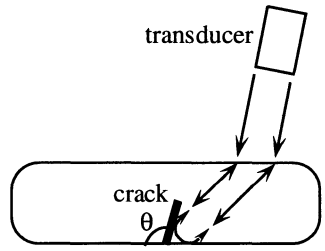

Figure 2. Illumination of a non-normal, surface-breaking crack by a transducer.

at points on the crack face. These fields were evaluated using the Gauss-Hermite beam model [5-7]. This approximate, paraxial model has the advantage of being computationally fast while accounting for focusing and beam spread effects, and it can be adapted to a wide variety of multi-layered geometries. The Gauss-Hermite beam model can predict the ultrasonic field radiated into isotropic and anisotropic materials through planar or simply curved interfaces by focused or unfocused transducers. After the beam model and Kirchhoff approximation are applied to find the total fields on the crack surface, numerical methods are used to evaluate the integral in Eq. (2).

EXPERIMENTAL SETUP AND PROCEDURES

The generation of actual surface-breaking cracks at a variety of angles is extremely difficult. Angled sawcuts could be used to simulate such cracks, but in the present work an even simpler approach was adopted for testing the model predictions. Since a large crack effectively acts as a corner-trap reflector, we simply replaced the crack with a different corner trap, namely the corner of an aluminum block cut at an oblique angle and immersed in water (Fig. 3). Rather than making one aluminum block for each angle of interest, a single test block was manufactured containing a series of reflecting surfaces, as illustrated in Fig. 4. The finished block measured 13.5" in the X direction, 5" in the Y direction, and was 1.5" thick. Along the X direction there were nine corner traps, each of length 1.5", and having $\theta = 90^{\circ}, 91^{\circ}, 92^{\circ}, \ldots 98^{\circ}$, respectively. By turning the specimen upside down so as to use the complementary angles, measurements could be made for $\theta = 90^{\circ}, 89^{\circ}, 88^{\circ}, \ldots 82^{\circ}$ as well.

The longitudinal wave (L-wave) speed in the Z direction of the test block was determined by measuring the time delays between successive back-surface echoes using a 5-MHz, 1/4" diameter, planar immersion transducer with its beam normal to the entry surface. A similar shear wave velocity measurement was made using a 5-MHz, 1/4" diam-

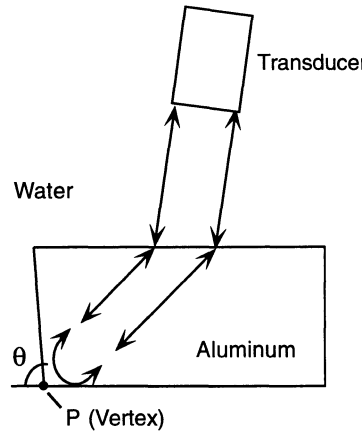

Figure 3. Reflection of the ultrasonic beam from a corner of the test block.

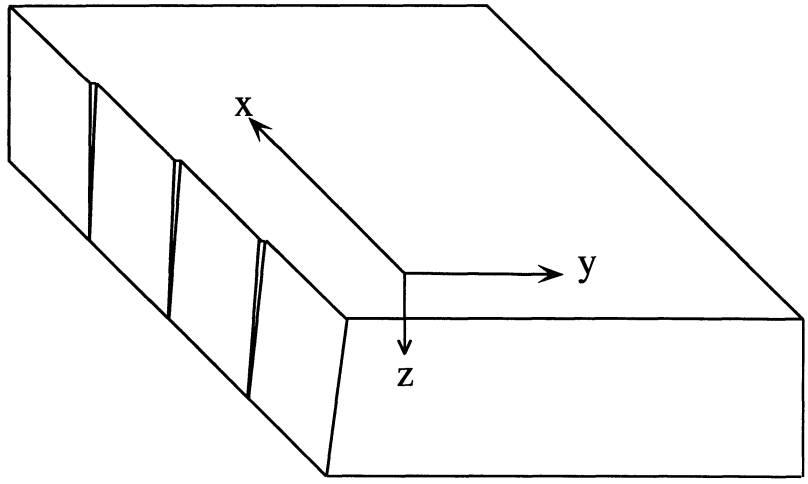

Figure 4. Schematic drawing of the aluminum test block with portions of one side cut at different angles. (The actual block contained cuts at nine angles.)

eter, contact probe. The longitudinal and shear velocities were found to be 0.639 and 0.318 cm/μsec, respectively. The shear wave velocity was found to vary by about 0.5 % depending on the polarization direction, indicating some degree of preferred alignment (texture) of the aluminum grains in the block. The shear velocity value cited above is for polarization along the Y direction. The L-wave attenuation for propagation in the Z direction was determined by comparing the spectral magnitudes of back-surface echoes from the aluminum block to those of a fused-quartz reference block. The measurement procedure is described in Ref. 8. The measured attenuation coefficient was approximately proportional to the square of the frequency and had a value of 0.012 Nepers/cm at 5 MHz. This level of attenuation would cause a 45° L-wave corner trap echo to be reduced by about 4% (at 5 MHz) relative to a normal-incidence, back-surface echo.

The same broadband immersion transducer used for the L-wave velocity and attenuation measurements was also used to measure corner-trap responses as functions of tilt angle (θ), lateral transducer position (Y), and frequency (f). The measurement geometry was that of Fig. 3 with a one-way water path of 5.0 cm for the central ray. The transducer was located on a computer-controlled bridge which permitted automatic scanning in the X and Y directions, The angle of incidence in water was set to 9.46°, leading to a 45.0° L-wave in the aluminum block. For each corner trap angle, the lateral position of the transducer was adjusted so that the central ray of the transducer aimed directly at the corner vertex (i.e., at point P in Fig. 3) when the scan coordinate read Y=0. This was accomplished by placing a small spherical reflector at a known location on top of the aluminum block, and using the peak echo from the sphere to locate the transducer's central ray in water. The known geometry of the aluminum block was then used to determine the proper Y=0 position, assuming a precise 45° L-wave in the block. This procedure was believed to be accurate to within 0.1 cm. The transducer was then scanned from Y = -1.27 cm to Y= +1.27 cm in steps of 0.0635 cm (0.025"), and at each transducer position the corner-trap echo was digitized, its FFT was computed, and spectral magnitudes were stored at selected frequencies within the transducer's bandwith. The microstructure of the specimen produced variations in the corner-trap echo when the probe was scanned in the X-direction. Similar minor variations had been noted for the back-surface echo under movement in either X or Y. To reduce the impact of such variations on the measured corner-trap echoes, at each position Y the probe was scanned in X over a 0.5" interval, and the spectral amplitudes were averaged. For normalization purposes, the spectral components of the normal-incident, back-surface echo (averaged over X and Y) were also measured.

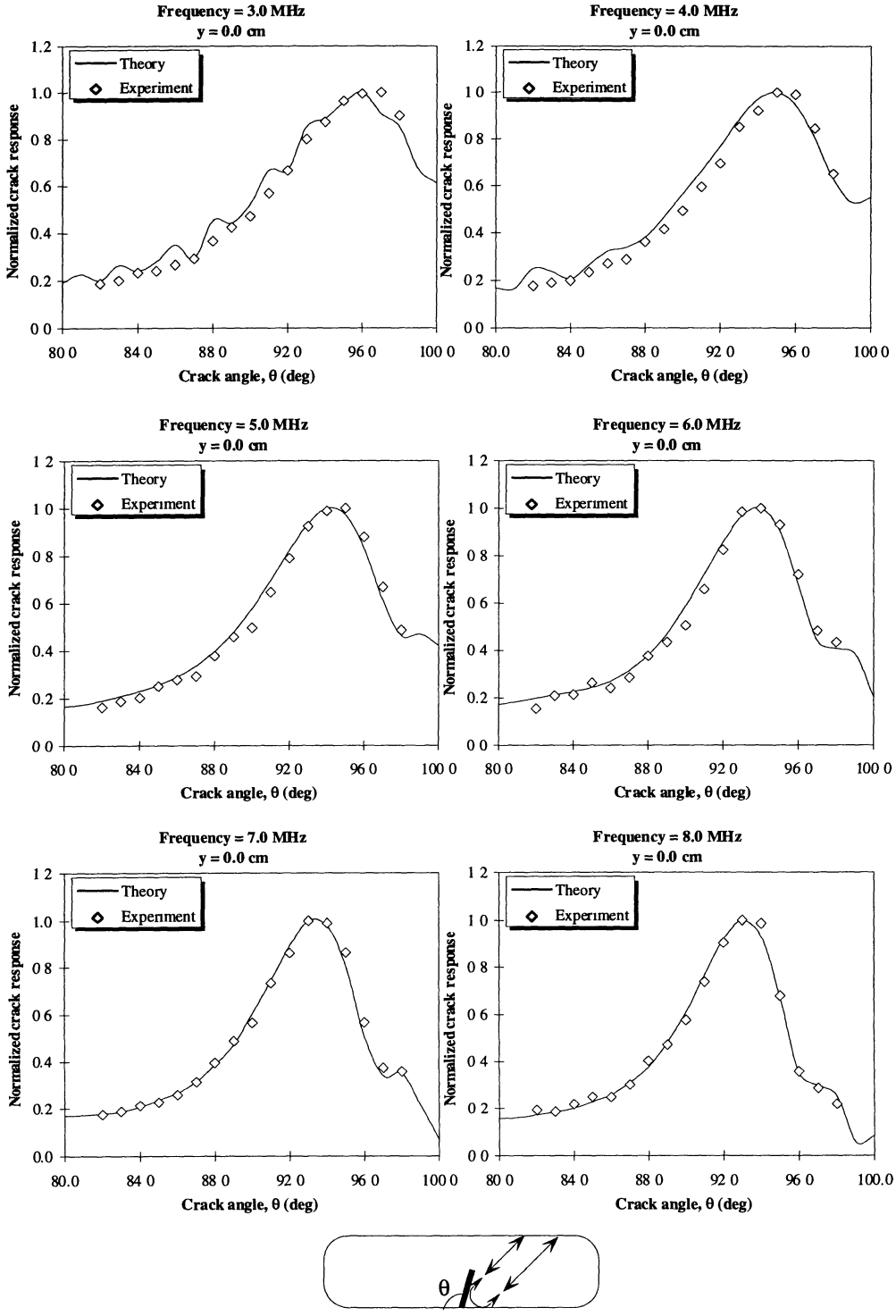

Figure 5. Measured and predicted corner-trap responses (simulated crack responses) at six frequencies, as functions of the tilt angle θ for a 45° L-wave inspection. The beam's central ray is aimed at the corner-trap vertex (Y=0).

EXPERIMENTAL RESULTS AND MODEL PREDICTIONS

In the preliminary applications of the model, we attempted to predict the ratio of like spectral magnitudes, (corner-trap echo)/(back-surface echo), as functions of θ, Y, and f. The model predictions tended to be consistently low by about 30% when compared with experiment. The reason for this is unknown, and is a topic of on-going research. It may be that the microstructure of the textured aluminum block affects corner-trap and back-surface echoes to different degrees. However, we found that the model was able to predict with reasonable accuracy the functional dependence of the corner-trap response on tilt angle, probe location and frequency. Thus when comparing model and experiment in the ensuing figures, we have simply normalized the measured and predicted peak response at each frequency to unity.

Fig. 5 displays the corner-trap (simulated crack) response verses the crack's tilt angle for selected frequencies between 3 and 8 MHz. The dependence on tilt angle is seen to be well predicted by the model. One might expect the response to be maximized for a normal crack ($\theta = 90^{o}$), but this is not the case for a diverging sound beam. Rather, the peak response occurs when the crack is tilted toward the transducer ($\theta > 90^{o}$), with the peak angle appearing to slowly approach 90^{o} as the frequency increases. This behavior is likely caused by a focusing effect that a tilted crack has on the sonic beam. As illustrated in Fig. 6, the pulse-echo response is approximately equivalent to a pitch-catch response in a geometry where the bottom reflecting surface is removed, and the crack is extended by adding its mirror image with respect to that surface. Thus, at a tilt angle (θ) of more than 90°, the extended crack is seen to resemble a concave mirror which has the effect of focussing the reflected beam on the receiver and consequently increasing the crack response.

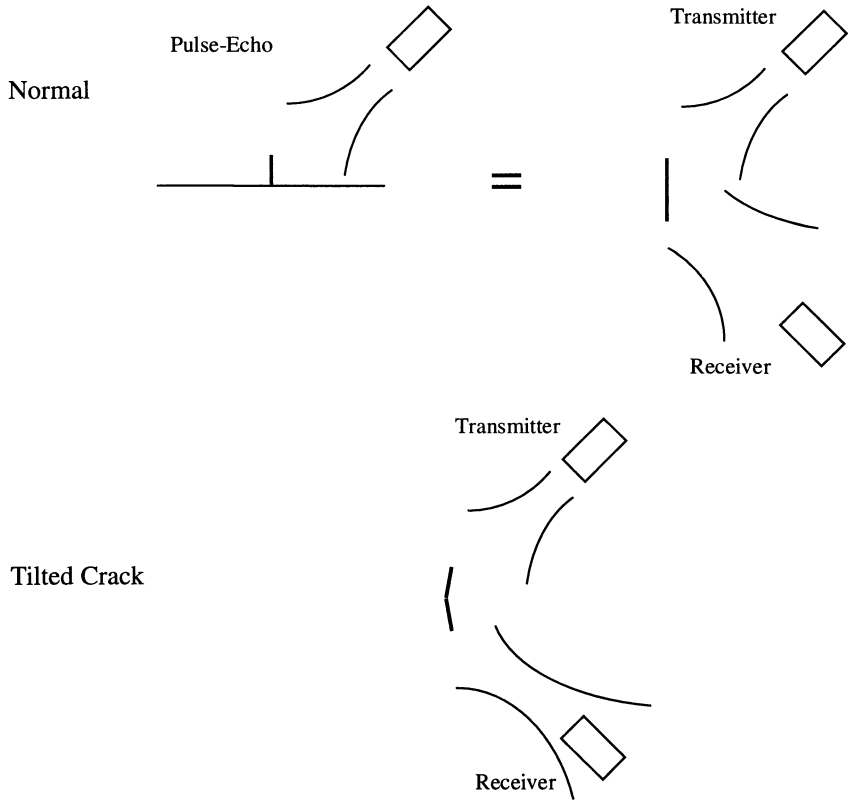

Figure 6. Schematic illustration of the approximate equivalence between pulse/echo and pitch/catch geometries, and the associated focusing effect of a tilted crack on a corner-reflected beam.

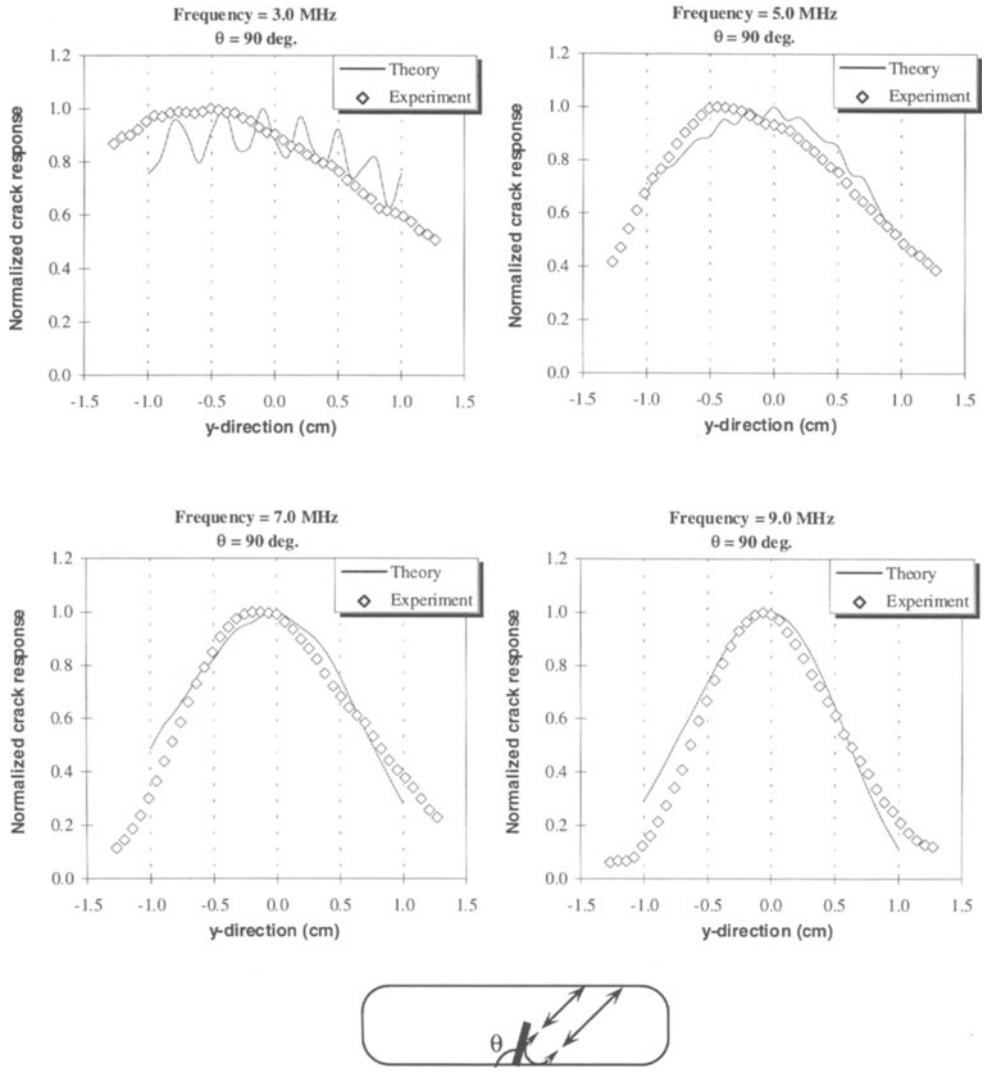

Figure 7. Corner-trap response (simulated crack response) as a function of lateral probe position for a normal reflector ($\theta = 90^{o}$).

Another interesting finding is that for a fixed crack angle, the maximum response does not occur when the central ray is aimed at the corner-trap vertex. For the $\theta = 90°$ case, Fig. 7 shows the variation of the simulated crack response when the transducer is scanned in the Y direction. The peak response occurs at $Y < 0$, i.e., with the central ray aimed at the vertical reflecting surface in Fig. 3 rather than at the vertex. This effect, which is seen to be enhanced at lower frequencies, is not presently understood. The model calculations reproduce the general shapes of the response-vs-position curves, but contained more structure than was seen experimentally.

CONCLUSION

In this study, the ultrasonic response from non-normal, surface-breaking cracks and similar corner reflectors were modeled using a formalism based on Auld's reciprocity relationship and the Kirchhoff approximation. To validate the model, experiments were performed to measure the pulse/echo response from a corner trap in an aluminum block.

The model did a good job of predicting the dependence of the corner-trap response on tilt angle, lateral transducer position, and frequency. The model was less sucessful in predicting the absolute magnitude of the corner-trap response relative to a normal-incidence, back-surface reflection.

The experimental measurements were carried out using a 5 MHz, 1/4" diameter, broadband, planar, immersion transducer. The (simulated) crack response was found to be quite sensitive to the crack angle and to the lateral position of the transducer relative to the crack vertex. As expected, the sensitivity to both crack angle and probe position increased with increasing frequency. The maximum response was not seen when the crack was normal to the surface, but rather when the corner trap angle θ in Fig. 3 was $> 90^{o}$. Such a geometry acts to focus the reflected sound beam and heighten the pulse/echo response. In addition, for a fixed crack angle, the maximum response did not necessarily occur when the central ray was aimed at the corner-trap vertex. This phenomenon is not yet understood.

Our future research plan envisions further corner-trap measurements and associated model analyses, for both longitudinal and shear wave beams in the solid. We hope to further elucidate the focusing effects of non-normal cracks, and to understand why the crack response is not maximized when the central ray is aimed at the crack vertex. Experiments will also be performed in a microstrure-free material, such as fused quartz, to discover why the model was unable to accurately predict the absolute magnitudes of corner-trap echoes in the aluminum specimen.

ACKNOWLEDGMENT

This work was sponsored by the Electric Power Research Institute under agreement W02687-15.

REFERENCES

1. A. Minachi and R. B. Thompson, "Predictions of pulse-echo ultrasonic signals from inner wall cracks in BWR nozzles", Review of Progress in Quantitative Nondestructive Evaluation, Vol. 14A (1994): 139-146.
2. A. Minachi and R. B. Thompson, "Ultrasonic wave propagation through nozzles and pipes with claddings around their inner walls", Review of Progress in Quantitative Nondestructive Evaluation, Vol. 15A (1995): 307-314.
3. A. Minachi, M. S. Greenwood and R. B. Thompson, " Prediction of pulse-echo ultrasonic signals from cracks observed through an interface with a step discontinuity: Comparison with experiments", Review of Progress in Quantitative Nondestructive Evaluation, Vol. 14B (1994): 1861-1868.
4. B. A. Auld, "General Electromechanical Reciprocity Relations Applied to the Calculation of Elastic Wave Scatering Coefficients", Wave Motion. Vol. 1 (1979): 3-10.
5. R. B. Thompson, T. A. Gray, J. H. Rose, V. G. Kogan and E. F. Lopes. "The Radiation of Elliptical and Bicylindrical Focused Piston Transducer", The Journal of The Acoustical Society of America 82 (1987): 1818-1828.
6. B. P. Newberry and R. B. Thompson, "A Paraxial Theory for the Propagation of Ultrasonic Beam in Anisotropic Solids", The Journal of The Acoustical Society of America 85 (1989): 2290-2300.
7. A. Minachi, Z. You, R. B. Thompson and W. Lord, "Validity of the Gauss-Hermite Beam Model in an Anisotropic, Layered Medium, Comparison to the Finite Element Method", IEEE Transactions on Ultrasonics Ferroelectrics and Frequency Control, Vol. 40, No. 4, 1993. 8.
8. P. D. Panetta, F. J. Margetan, I. Yalda, and R. B. Thompson, " Ultrasonic attenuation measurements in jet-engine titanium alloys", Review of Progress in Quantitative Nondestructive Evaluation, Vol. 15B (1996): 1525-1532.